Vol. 211, No. 1, 1995 BIOCHEMICAL AND BIOPHYSICAL RESEARCH COMMUNICATIONS
June 6, 1995 Pages 198-204

EPR AND REDOX CHARACTERIZATION OF FERREDOXINS I AND II FROM *DESULFOVIBRIO VULGARIS* MIYAZAKI

Marcel ASSO[a], Omar MBARKI[a], Bruno GUIGLIARELLI[a],
Tatsuhiko YAGI[b] and Patrick BERTRAND[a*]

a- Laboratoire de Bioénergétique et Ingénierie des Protéines, UPR-CNRS 9036, et Laboratoire d'Electronique des Milieux Condensés, Université de Provence, Centre St Jérôme, 13397 Marseille cedex 20, FRANCE

b- Department of Chemistry, Shizuoka University, 836 Oya Shizuoka 422, JAPAN

Received April 18, 1995

Detailed redox titrations monitored by EPR and UV-visible spectroscopies have been carried out on the dimeric ferredoxins I and II from *Desulfovibrio vulgaris* Miyazaki. Ferredoxin II contains a unique [4Fe-4S] cluster per subunit characterized by a midpoint potential of -417 mV at 24°C. The enthalpic and entropic contributions to the redox free energy variation of this cluster have been determined from the temperature dependence of the midpoint potential and compared to the data reported for other iron-sulfur proteins. The molecular arrangement of the two subunits is such that two $[4Fe\text{-}4S]^{1+}$ clusters are magnetically coupled in the fully reduced state of the protein. Ferredoxin I contains one [3Fe-4S] and one [4Fe-4S] cluster per subunit, whose spectral and redox properties are very similar to those of the same clusters in ferredoxin III from *Desulfovibrio africanus*. The strong heterogeneity in the redox properties of the [3Fe-4S] center supports a bridging position between the N-terminal and C-terminal parts of the protein.

In bacteria of the genus *Desulfovibrio*, oxidation of organic substrates or molecular hydrogen is coupled to the dissimilatory reduction of sulfate. Cytochromes c_3 and ferredoxins are well known components of the electron transfer systems involved in this coupling, and constitute good models for the study of intermolecular electron exchange. However, owing to the specificity of these exchanges (1), such studies require a detailed characterization of proteins isolated from the same species.

In the bacterium *D. vulgaris* Miyazaki, the redox properties of the cytochrome c_3 have been studied in detail (2,3) and its crystal structure has been reported(4). Two ferredoxins, Fd I and Fd II, have been isolated from this

*To whom correspondence should be addressed. Fax: (33) 91 28 86 50.

0006-291X/95 $5.00

bacterium, which have been only partly characterized by physico-chemical techniques (5). Fd I and Fd II were purified as homodimer of Mr 12,000 and Mr 14,000 respectively, and both contain 7 cysteine residues per monomer (6,7). However, their difference in iron and sulfur contents indicated different iron-sulfur cluster composition (6,7).

In this work, we report detailed redox titrations of ferredoxins I and II from *D. vulgaris* Miyazaki monitored by EPR and optical spectroscopies, which gives a complete view on the nature, the stoichiometry and the redox characteristics of their Fe-S centers. The properties of these proteins are compared to those reported for other ferredoxins.

MATERIAL AND METHODS

Ferredoxins I and II from *D. vulgaris* Miyazaki were purified as previously reported (5).

The redox titrations were performed in a 100 mM Tris-HCl pH 7.7 solution kept under argon atmosphere as described in reference (8), in the presence of the following mediators : methylene blue, 2-hydroxy-1,4-naphtoquinone, benzyl viologen, phenosafranine and methyl viologen.

EPR spectroscopy and spin quantitation were carried out as in reference (8).

Optical titrations were performed on a DU 40 Beckman spectrophotometer by using a specially designed anaerobic cell. The absorbance was measured at 430 nm, where the absorbance variation of the Fe-S clusters is maximum, and where the contribution of mediators is negligible.

Variable temperature experiments were carried out according to the nonisothermal cell arrangement: the optical cell containing the protein solution, a Pt electrode and a calibrated thermocouple was placed in a variable temperature holder. This cell was connected through a flexible KCl (3M) salt bridge to an Ag/AgCl-KCl (3M) reference electrode maintained at 24°C (+208mV *vs* NHE). In these conditions, if the midpoint potential E_m measured between the two electrodes is corrected for the thermal junction potentials, the coefficient dE_m/dT is proportional to the entropy variation ΔS_{RC} of the studied redox couple (9). In the temperature range 8°C-46°C, the protein stability was checked over several hours, and the sum of the junction potentials was found to vary from 3mV to 7mV by replacing the protein solution by the buffer solution. The entropic and enthalpic contributions ΔS and ΔH for the complete cell reaction adjusted to NHE scale are given by (9):

$$\Delta G = -\mathcal{F} \cdot E_m \quad ; \quad \Delta S = \Delta S_{RC} - 65.2 \ JK^{-1}mol^{-1}; \quad \Delta H = \Delta G + T \cdot \Delta S \ .$$

RESULTS

Ferredoxin II : In the as isolated state, Fd II gives a weak (<0.1 spin/monomer) $[3Fe\text{-}4S]^{1+}$ EPR signal centered at g = 2.01, which disappears at potentials more negative than -200mV (Fig.1). On subsequent reduction, a typical $[4Fe\text{-}4S]^{1+}$ EPR signal appears at g=2.06, 1.94 and 1.90 (Fig.1c). At very negative potentials, this spectrum becomes more complex, exhibiting a splitting of the g=1.94 line and broad lateral lines at g=1.83 and 2.12 (Fig.1d). At -500mV, this signal corresponds to 0.9 ± 0.1 spin/monomer. The intensity variations of the $[4Fe\text{-}4S]^{1+}$signal as a function of the redox

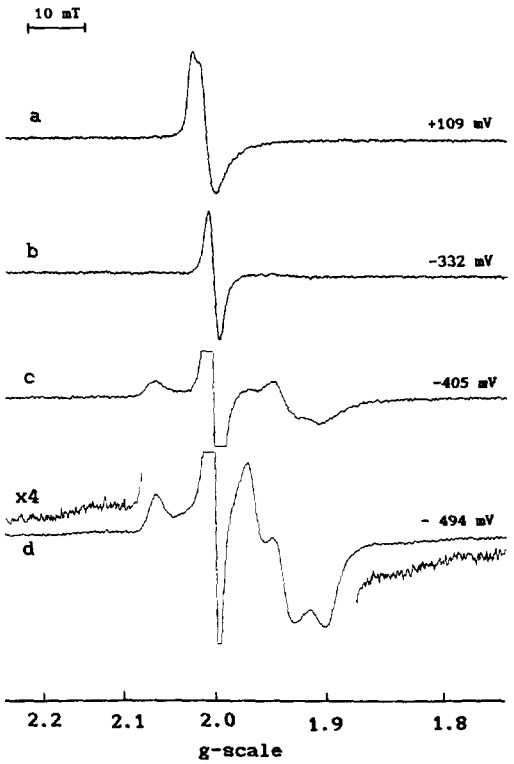

Figure 1 . Representative EPR spectra of *D. vulgaris* Miyazaki ferredoxin II during the redox titration.
Experimental conditions: temperature, 15K; microwave power, 0.4mW; microwave frequency, 9.303 GHz; modulation frequency, 100 kHz; modulation amplitude, 0.5 mT. The g = 2 signal visible in b, c, and d arises from mediators.

potential are well fitted to a nernstian curve centered at -417mV (Fig.2). An optical titration carried out at the same temperature (24°C) gave essentially the same result (Fig.2).

In order to determine the enthalpic and entropic contributions to the redox free energy of the [4Fe-4S] center, we measured the temperature dependence of its midpoint potential E_m by optical titrations performed in a nonisothermal configuration. The advantage of this method is that it gives directly the entropy variation ΔS_{RC} relative to the redox couple of interest. The variations of E_m in the range 8°C-46°C are shown in figure 2. In this temperature range, E_m decreases with a slope of -0.40 ± 0.10 mV/K which leads to ΔS_{RC} = - 38 ± 10 $JK^{-1}mol^{-1}$. From these data we deduced:

ΔS = -103 ± 10 $JK^{-1}mol^{-1}$ and ΔH = 9.65 ± 3 kJ mol^{-1} at 24°C.

Ferredoxin I : In the as isolated state, this protein gives a typical $[3Fe\text{-}4S]^{1+}$ EPR signal centered at g=2.01, which corresponds to 0.9±0.1 spin/monomer (Fig.3a). Upon reduction with dithionite, the disappearance of

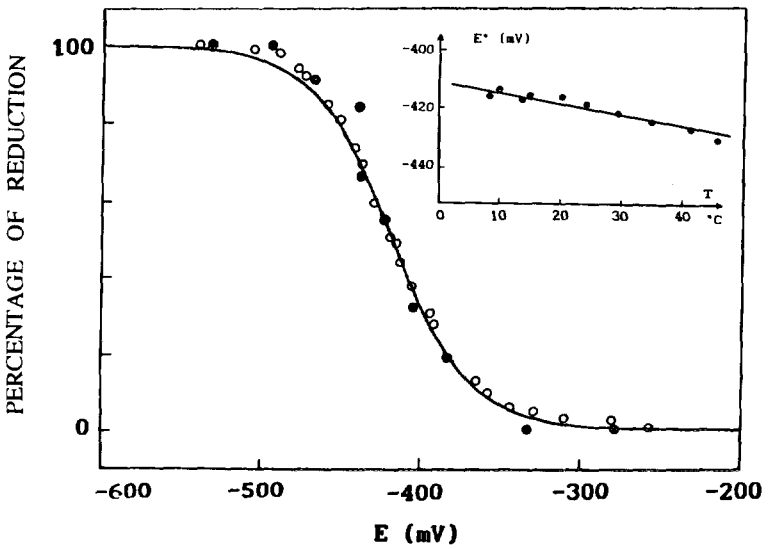

Figure 2 . Redox titration of *D. vulgaris* Miyazaki ferredoxin II at 24°C.
● Normalized integrated intensity of the EPR signal. O ,Percentage of reduction deduced from absorbance measurements at 430 nm.
The solid line is a Nernst curve centered at -417 mV.
Inset: Temperature dependence of the [4Fe-4S] center midpoint potential. The slope of the straight line is -0.40 mV/°C.

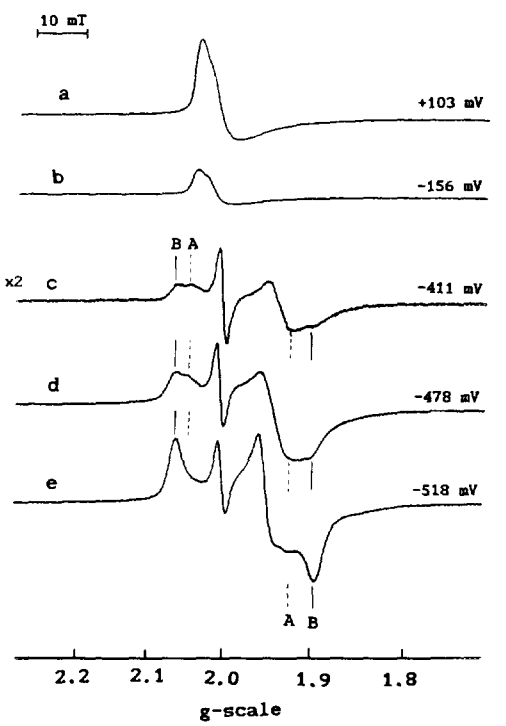

Figure 3 . Representative EPR spectra of *D.vulgaris* Miyazaki ferredoxin I during the redox titration.
Experimental conditions as for figure 1 except for temperature, 12.5 K, and microwave power, 1 mW.

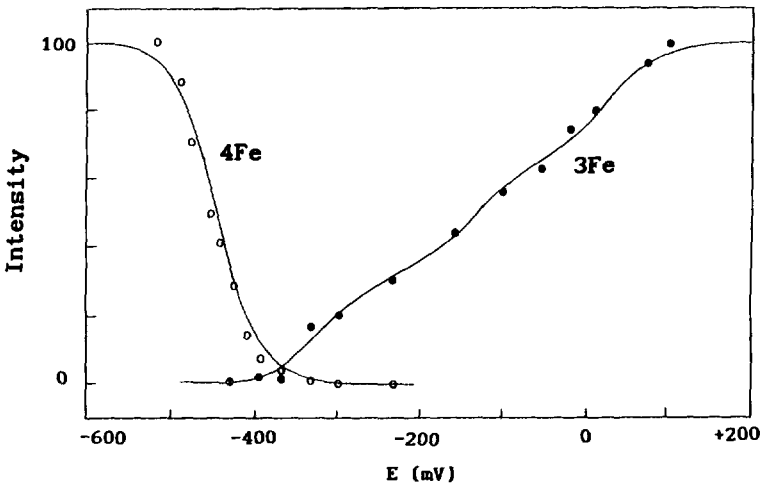

Figure 4 . Redox titration of the EPR signals given by ferredoxin I. Normalized integrated intensity of the $[3Fe\text{-}4S]^{1+}$ (●) and $[4Fe\text{-}4S]^{1+}$ (O) EPR signals. Same conditions as for figure 3. The full lines represent the superposition of three Nernst curves centered at 40mV, -140mV and -310mV for the [3Fe] center and a unique Nernst curve centered at -440mV for the [4Fe] center.

this signal spread out between +100mV and -350mV, and the variation of its intensity as a function of the potential can be described by the superposition of at least three different Nernst curves (Fig.4). This reveals a marked heterogeneity of the redox properties of this [3Fe-4S] cluster.

Below -350mV, a composite spectrum comprising two components A and B, with features at g=2.044, 1.948, 1.920 and g=2.062, 1.948, 1.898 characteristic of $[4Fe\text{-}4S]^{1+}$ centers, is observed (Fig.3). In the fully reduced state (Fig.3e), the integrated intensity of the whole $[4Fe\text{-}4S]^{1+}$ spectrum corresponds to 1.2±0.1 spin/monomer, and the intensity ratio A/B was estimated to about 1:4 by spectral simulation. The total spin intensity of the spectrum titrates with a midpoint potential of -440mV (Fig.4) , the redox potentials of the two components A and B differing by about 20mV.

In an attempt to convert the [3Fe-4S] cluster into a [4Fe-4S] one, a Fd I sample poised at -350mV was anerobically incubated with ammonium ferrous sulfate for 15 min. After full reduction of the sample with dithionite and freezing, the EPR spectrum showed no change in the g=2 region when compared to that given in figure 3e, but a broad peak appeared in the g=5 region. Its amplitude was weak and did not increase after subsequent addition of Fe^{2+} ions or lenghtening of the incubation time.

DISCUSSION

In spite of the same number of cysteine residues, Fd I and II from *D. vulgaris* Miyazaki exhibit different Fe-S contents. The small amount of [3Fe-4S]

clusters found in Fd II is likely due to a limited oxidative damage during the purification. The spectral and redox properties of this ferredoxin clearly show that it contains only one [4Fe-4S] center per monomer, with a midpoint potential of -417mV at 24°C. This confirms the similarity of Fd II with Fd I from *D. africanus* and with Fd I from *D.desulfurican* Norway, as indicated by sequence comparisons (7). However, the complex EPR spectrum shown by the fully reduced Fd II is reminiscent of those given by the two spin-coupled $[4Fe-4S]^{1+}$ centers of clostridial ferredoxins (10) or of photosystem I (11). This indicates that the $[4Fe-4S]^{1+}$ centers belonging to the two subunits of the Fd II dimer are closely spaced (1.0-1.2nm)(11) and interact magnetically. To our knowledge, this constitutes the first evidence of an intermonomer spin-spin coupling in a multimeric ferredoxin.

The determination of the enthalpic and entropic contributions to the redox free energy is essential for understanding the factors which modulate the redox potential of Fe-S proteins. The values we found for the $[4Fe-4S]^{2+,1+}$ couple in Fd II can be compared to the few data available for other Fe-S proteins: ΔS_{RC} = -42 $JK^{-1}mol^{-1}$, ΔH = -66 $kJmol^{-1}$ for the $[4Fe-4S]^{3+,2+}$ couple in *Chromatium vinosum* high potential iron-sulfur protein (HIPIP) (9), and ΔS_{RC} = -207 $JK^{-1}mol^{-1}$, ΔH = -57 $kJmol^{-1}$ for the $[2Fe-2S]^{2+,1+}$ couple in adrenodoxin (12). The similar ΔS_{RC} values measured for HIPIP and Fd II shows that the 760mV difference between their potentials is essentially due to enthalpic effects. According to recent theoretical calculations, these effects arise from valence delocalization and antiferromagnetic spin coupling contributions which are internal to the cluster (13), and from the interaction of the cluster with its surrounding (14). The negative values of ΔS_{RC} may be related to an extra ordering of the solvent molecule in the reduced state, an effect which is very dependent on the accessibility of the redox site to the solvent (14). Thus, our results suggest that the solvent accessibility to the [4Fe-4S] cluster is similar in Fd II and in HIPIP.

In the as isolated state, Fd I carries one [3Fe-4S] and one [4Fe-4S] cluster per monomer. This Fe-S composition is identical to that of the homologous Fd III from *D. africanus* (*D.a.*FdIII) which also contains 7 cysteine residues per monomer (15). The $[4Fe-4S]^{1+}$ cluster of FdI gives a composite EPR spectrum, a feature previously reported for *D.a.*FdIII (15) and for other ferredoxins (16), and its redox potential of -440mV is close to the value of -410mV measured electrochemically for the [4Fe] center of *D.a.*FdIII (15). The redox behavior of the [3Fe] center of FdI presents a strong heterogeneity, an effect already observed for [3Fe] clusters in other proteins (8,16). In *D.a.*FdIII, some properties of the [3Fe] center are also peculiar, like the solvent dependent shape of its EPR signal and its low and variable spin intensity (15). These properties suggest that in both proteins, the [3Fe] binding site can undergo

significant conformation changes, in agreement with the proposed coordination by Cys11, Cys 17 and Cys 51, in a bridging position between the N-terminal and C-terminal parts of the protein (15). When Fd I is incubated with Fe^{2+} ions in reducing conditions, no conversion of the $[3Fe-4S]^{0}$ cluster into a $[4Fe-4S]^{1+}$ cluster with spin S=1/2 occurs, which is likely due to the lack of a Cys residue in position 14 in the sequence. However, the appearance of a g=5 EPR signal, as observed in similar conditions with *D.a.*FdIII (17) and with *Pyrococcus furiosus* ferredoxin (18), indicates that the interconversion of the [3Fe-4S] center takes place, leading to a $[4Fe-4S]^{1+}$ cluster with a S=3/2 spin state arising from a non-cysteinyl coordination of one iron site. As proposed for *D.a.*FdIII (15), the aspartic acid at position 14 of the FdI sequence could be the fourth ligation site of this mixed ligand [4Fe-4S] cluster.

The different Fe-S composition of Fd I and Fd II from *D. vulgaris* Miyazaki could be related to different functional role. Both these proteins function as electron carriers between pyruvate dehydrogenase and cytochrome c_3 , but the efficiency of Fd II is 40% less than that of Fd I, suggesting that Fd II may be involved in reaction with other proteins (7).

REFERENCES

1. Capeillère-Blandin, C., Guerlesquin, F. and Bruschi, M. (1986) Biochim. Biophys Acta, 848, 279-293.
2. Benosman, H., Asso, M., Bertrand, P., Yagi, T. and Gayda, J.P. (1989) Eur. J. Biochem., 182, 51-55.
3. Fan, K., Akutsu, H., Kyogoku, Y. and Niki, K. (1990) Biochemistry, 29, 2257-2263.
4. Higuchi, Y., Kusunoki, M., Matsura, Y., Yasuoka, N. and Kakudo, M. (1984) J. Mol. Biol., 172, 109-139.
5. Ogata, M., Kondo, S., Okawara, N. and Yagi, T. (1988) J. Biochem., 103, 121-125.
6. Okawara, N., Ogata, M., Yagi, T., Wakabayashi, S. and Matsubara, H., (1988) J. Biochem., 104, 196-199.
7. Okawara, N., Ogata, M., Yagi, T., Wakabayashi, S. and Matsubara, H., (1988) Biochimie, 70, 1815-1820.
8. Asso, M., Guigliarelli, B., Yagi, T. and Bertrand, P. (1992) Biochim. Biophys. Acta, 1122, 50-56.
9. Taniguchi, V.T., Sailasuta-Scott, N., Anson, F.C. and Gray, H.B. (1980) Pure and Appl. Chem., 52, 2275-2281.
10. Moulis, J.M., Auric, P., Gaillard, J. and Meyer, J. (1984) J. Biol. Chem., 259, 11396-11402.
11. Guigliarelli, B., Guillaussier, J., More, C., Setif, P., Bottin, H. and Bertrand, P. (1993) J. Biol. Chem., 268, 900-908.
12. Huang, Y.Y. and Kimura, T. (1983) Anal. Biochem., 133, 385-393.
13. Mouesca, J.M., Chen, J.L., Noodleman, L., Bashford, D. and Case, D.A. (1994) J. Am. Chem. Soc., 116, 11898-11914.
14. Langen, R., Jensen, G.M., Jacob, V. Stephens, P.J. and Warshel, A. (1992) J. Biol. Chem., 267, 25625-25627.
15. Armstrong, F.A., George, S.J., Cammack, R., Hatchikian, E.C. and Thomson, A.J. (1989) Biochem. J., 264, 265-273.
16. Guigliarelli, B., Bertrand, P., More, C., Papavassiliou, P., Hatchikian, E.C. and Gayda, J.P. (1985) Biochim. Biophys. Acta, 810, 319-324.
17. George, S.J., Armstrong, F.A., Hatchikian, E.C. and Thomson, A.J. (1989) Biochem. J., 264, 275-284.
18. Conover, R.C., Kowal, A.T., Weiguang, F., Park, J.B., Aono, S., Adams, M.W.W., Johnson, M.K., (1990) J. Biol. Chem., 265, 8533-8541.